

## Intense field dynamics of H<sub>2</sub> and D<sub>2</sub> with few-cycle laser pulses

J McKenna, B Srigengan, I D Williams

Department Pure and Applied of Physics, Queen's University Belfast, Belfast, BT7 1NN, UK

J Wood, E M L English, W A Bryan, W R Newell

Department of Physics and Astronomy, University College London, London, WC1E 6BT, UK

I C E Turcu

Central Laser Facility, CCLRC Rutherford Appleton Laboratory, Chilton, Didcot, Oxon., OX11 0QX, UK

Main contact email address: jarlath.mckenna@qub.ac.uk

### Introduction

As the most fundamental and simplistic molecular system, the H<sub>2</sub><sup>+</sup> ion is by far the most alluring in intense field studies both from a theoretical and an experimental viewpoint. Despite however the vast amount of knowledge accumulated through numerous studies<sup>1)</sup>, a full understanding of its dissociation and ionization dynamics is far from complete.

Whilst production of H<sub>2</sub><sup>+</sup> is generally achieved via ionization of the neutral H<sub>2</sub> target on the rising edge of the laser pulse, this method may in itself present added complexity to the study. This is due to an uncertainty in the nature of how H<sub>2</sub><sup>+</sup> is formed i.e. its vibrational population distribution. Unquestionably this aspect is sensitive to initial field conditions, largely the laser intensity at the point of production<sup>2)</sup>, photon wavelength<sup>3)</sup> and duration of the ionizing pulse. This may cloud the interpretation of the H<sub>2</sub><sup>+</sup> dissociation dynamics. One method of avoiding this obstacle is to start with a primary H<sub>2</sub><sup>+</sup> target, produced for example from e-impact in a discharge ion source (a method we have implemented in recent studies<sup>4,5)</sup>). This thereby guarantees a Frank-Condon distribution of states, and most importantly does not vary as laser parameters are changed. However such studies are not trivial due to systematic difficulties and have thus far been limited<sup>4-6)</sup>.

Apart from ease as a target, H<sub>2</sub> does hold the appeal that extraction of the proton signal produced potentially displays the full range of phenomena relevant to these studies. These fundamental processes include bond softening<sup>7)</sup> and hardening<sup>8)</sup> (or vibrational trapping evidenced by zero-photon dissociation), laser induced alignment along the field polarization direction<sup>9)</sup>, charge-resonantly enhanced ionization<sup>10)</sup> (CREI) at a critical internuclear separation<sup>11,12)</sup> and nonsequential double ionization effects from laser-driven electron rescattering events<sup>13,14)</sup>.

Perhaps the most growing interest in recent studies has been the use of few-cycle laser pulses as the molecular probe. A vast improvement in laser technology and more importantly optical methods has been key with developments now approaching the limit of single-cycle phase-locked pulses. This would enable very precise control of both nuclear and electron motion with the capacity to study events on an even shorter timescale (molecular clock<sup>13)</sup>). The duration of the pulse interaction is critical, particularly in the case of H<sub>2</sub> and D<sub>2</sub>, as those shorter than the vibrational period (~20fs) result in inertially confined molecules during the ionization event<sup>15)</sup> removing the smearing due to vibrational motion.

To this end, we present here the first measurements using the newly developed 10fs laser system at RAL (UK) Astra laser facility (TA1). The results targeting H<sub>2</sub> and D<sub>2</sub> are in the preliminary stage of analysis and so for the purposes of this report only a brief overview will be presented. We have looked at the effect that varying the pulse duration from 12fs to 50fs (via spectral broadening) has on the main features of time-of-flight (TOF) spectra from D<sub>2</sub> (namely dissociation and coulomb explosion peaks). We have also scanned the interaction with H<sub>2</sub> as a function of focal intensity using an intensity selective scan (ISS) technique<sup>16,17)</sup> and moreover observed the variation of features as the laser polarization direction was rotated.

### Experimental Configuration

For the current study, TOF momentum spectroscopy has been used to detect the ionization events. The experimental arrangement consisted of a conventional time-of-flight spectrometer, described in detail in previous CLF Annual Reports<sup>18,19)</sup>. The spectrometer was operated at a tank pressure of 1.5x10<sup>-7</sup> mBar for both H<sub>2</sub> and D<sub>2</sub>, low enough to avoid space-charge effects<sup>20)</sup>. Ionic products, extracted through a small aperture (0.25mm diameter), are detected by a set of micro-channel plates with the TOF recorded via a fast digital storage oscilloscope. Wiley-McLaren<sup>21)</sup> conditions have been used to give good forward and backward resolution of dissociative peaks.

The ultrashort (~10 femtosecond) pulses generated by Astra TA1 at 10Hz repetition rate are produced by employing a hollow-fibre optical technique<sup>22)</sup>. Only a brief outline of the setup is described here but for more details see Turcu *et al.*<sup>23)</sup>. From the output of a Ti:sapphire regenerative amplifier (centred at 800nm, bandwidth 30nm) the longer pulses are compressed to 40fs by chirped-pulse amplification in a conventional grating compressor. The output from this is then coupled into a hollow-core fibre (250µm diameter, 1m long) filled with purified argon to a pressure differential (PD) of 0.3atm along the fibre length. In propagation down the fibre, the input pulses are spectrally broadened to ~100nm bandwidth (FWHM). Compression of these using a set of 10 chirped mirrors (allowing for compensation for propagation through the spectrometer input window) produces pulses of 10-12fs at the point of interaction with the gas target. The collimated pulses before focusing (10mm diameter) have an energy of 400µJ. After back-focusing with a 75mm focal length spherical mirror a peak intensity of 4x10<sup>15</sup> Wcm<sup>-2</sup> is achieved. A check on this intensity was made by performing a calibration using a Xe gas target. Traces of up to Xe<sup>7+</sup> were observed confirming the interaction intensity. The linearly polarized pulses ordinarily have their polarization vector aligned along the spectrometers detector axis although for the polarization angle variation measurement, a half-waveplate (0.3mm thickness) was inserted. The focal mirror could be translated in x and y to maximize the focal overlap with the target and also along z, the direction of laser propagation, so as to extract ions from different intensity regions of the focus. This is the principal of the ISS method used for precise control on variation of the laser intensity at interaction.

### I. Variation of pulse duration

Displayed in Figure 1 are the forward peaks of the TOF spectra from a D<sub>2</sub> target using linearly polarized light orientated along the detector axis. The four cases (a)-(d) represent variation of the laser pulse duration by control of the spectral broadening of the pulses through variation of the internal fibre PD. The pulse durations are 50fs, 12fs, 35fs and 50fs for (a)-(d) respectively achieved through PDs of 0.0atm, 0.3atm, 0.6atm and 1.0atm. In the case of PD of 0.3atm this provides the optimum conditions for minimization of the pulse duration. Figures 1(c) and 1(d)

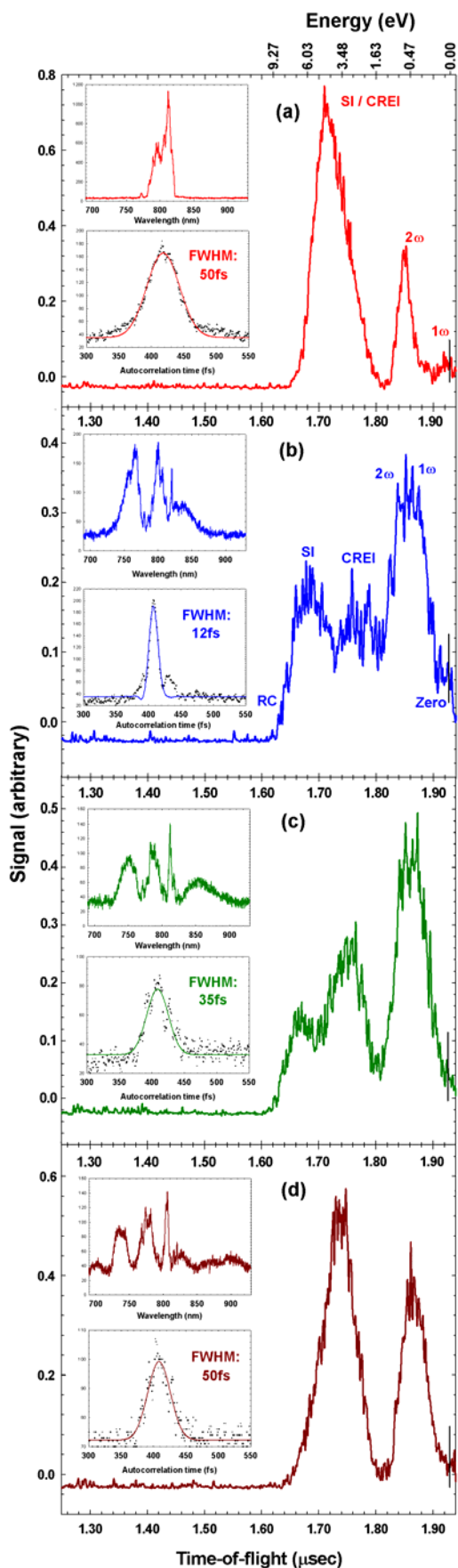


**Figure 1.** Forward peaks of  $D^+$  time-of-flight spectra from a  $D_2$  target. The results are from variation of the hollow-fibre pressure differential (PD) resulting in a change of pulse length ( $\tau$ ). For (a) PD=0.0atm,  $\tau=50$ fs (b) PD=0.3atm,  $\tau=12$ fs (c) PD=0.6atm,  $\tau=35$ fs (d) PD=1.0atm,  $\tau=50$ fs. The insets of the figures show the corresponding wavelength spectra (top) and autocorrelation measurement (bottom).

thus represent over-broadened pulses. The peak intensities have not been normalized for each case hence accounting for a small variation in the output pulse energy, the respective (a-d) interaction intensities are  $1.5 \times 10^{15} \text{ Wcm}^{-2}$ ,  $4.0 \times 10^{15} \text{ Wcm}^{-2}$ ,  $1.2 \times 10^{15} \text{ Wcm}^{-2}$  and  $8.5 \times 10^{14} \text{ Wcm}^{-2}$  (allowing for the change in pulse duration). Shown in the insets of each figure are the fibre output wavelength spectral profiles (top) and the corresponding autocorrelation measurement (bottom) after pulse compression (fitted with a gaussian profile).

The contrast in TOF spectra for the two pulse duration extremes (50fs (a) and 12fs (b)) is stark. The spectral shape of the long pulse duration is similar to that observed elsewhere<sup>24</sup>. The low-energy peaks may be interpreted as due to bondsoftening (BS) dissociation, the one centred at zero-energy arising from 1-photon ( $1\omega$ ) dissociation. This is understood in terms of light-dressed potential curves shifted by a photon of energy due to absorption of a single photon enabling higher lying vibrational states to ( $v = 5-9$ ) to flow out onto the repulsive potential. In a similar manner lower vibrational states ( $v = 0-4$ ) may dissociate through  $2\omega$  absorption peaked at 0.5 eV. The large peak at high energy is from sequential ionization (SI) to  $D_2^+$  which then coulomb explodes (CE) into two  $D^+$  ions. An enhancement in this process from charge resonance (CREI) occurs at a critical separation as the  $D-D^+$  ions move apart<sup>10,11</sup>.

Compression of the pulses to 12fs dramatically changes this high energy feature. Most notably a splitting of the peak is observed as seen in two very recent experiments employing 7fs<sup>25</sup> and 8.6fs<sup>15</sup> pulses. The outermost peak (4 - 10 eV) is believed to arise from the normal sequential process (SI) shifting inwards to merge with the inner CREI peak as the pulse length increases. Rudenko *et al.*<sup>25</sup> also display evidence that the inner peak is sensitive to the pulse shape, removing it when small ( $\sim 15\%$  of main peak) pre- and post-pulses are eliminated. Some recollision-based (RC) ionization (double ionization resulting from rescattering of the first removed electron) is also expected to result, extending the trailing edge of the highest energy peak up to 10eV. We however have not resolved these events from the SI process and therefore can only postulate on their existence and shall make no further comment.

The second major difference is in the dissociation peaks. While the  $2\omega$  peak remains at similar energy as before, a second peak rises up on the low energy side to merge with it. Although the scatter from noise on the spectra shown does not enable resolution into two separate peaks, we have obtained other spectra showing a clear splitting of this dissociation structure similar to that seen by Rudenko *et al.*<sup>25</sup>. In their interpretation they designate it as the  $1\omega$  process which would therefore have shifted to higher energy and risen in prominence with decrease of pulse length. Moreover, whilst not reported by Rudenko *et al.*, we observe a further zero energy peak. Although it is only mildly discernable in the spectra of Figure 1(b), it becomes clearer as we rotate the laser polarization direction (still to be discussed). The origin of this feature is uncertain but it may result from zero-photon dissociation (ZPD), an aspect of bond-hardening (see Frasinski *et al.*<sup>8</sup>) for details). The difficulty in truly interpreting the data is the uncertainty of the initial state of the  $D_2^+$  ion. The question still remains as to whether the changes observed are due to population of a different distribution of vibrational states in producing the  $D_2^+$  ions using different pulse lengths, or do they arise from a change in the dissociative process itself.

An overall broadening in the  $1\omega$  and  $2\omega$  dissociation feature is consistent with the increase in spectral width. For the 50fs pulses in Figure 1(a), the wavelength spectra are sharply peaked around 800nm producing photons of well-defined energy, 1.55eV. The 12fs pulse on the other hand is constructed of photons typically in the 750-850 nm range resulting in a spread of photon energies from 1.46 – 1.66 eV. This serves to increase the range of vibrational states from which  $D_2^+$  ions may

dissociate giving an energy broadening of the dissociative features.

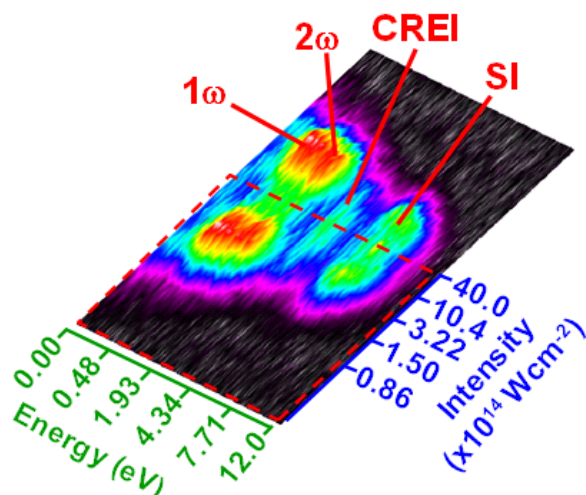


**Figure 2.** Colormap of  $H^+$  results from intensity variation using the ISS technique on a  $H_2$  target (displaying only the forward peaks). The results are plotted on a non-linear intensity scale. Also shown is the nonlinear energy scale corresponding to the fragmentation energy of the  $H^+$  ions. (See text for description of labeled peaks)

As the pulse duration was increased again through over-broadening, strongly apparent is the change in the CE feature. The branching ratio of the SI and CREI peaks reverses (Figure 1(c)) before they merge again into a single peak (Figure 1(d)) similar to the one seen in Figure 1(a). Curious is the fact that the dissociation peaks do not return to the long pulse structure of sharp  $1\omega$  and  $2\omega$  prominences but remain as a broad convolution merged as one. The broadening may still result from the range of photon energies in the pulse.

## II. Intensity variation

Although  $H_2^+$  and  $D_2^+$  are very similar, with the use of ultrashort pulses, small differences in vibrational structure and vibrational period may become significant. Therefore using  $H_2$  as the primary molecule, we performed an ISS to observe any intensity-dependent changes in the main features discussed. The results are shown in Figure 2 with the pulse duration optimized to 10fs. Largely these features show no dramatic variation to  $D_2^+$ . The  $1\omega$ ,  $2\omega$ , CREI and SI features are labeled as previously identified. The general form of the plot shows overall reduced signal at highest intensity due to extraction of ions from the laser focal centre (minimized volume) –see for example<sup>16</sup>). However despite this, we should note that the CREI process is still peaked and displays a rapid drop-off in signal with intensity decrease, much more so than either the dissociative or SI processes. The CREI process has therefore got a much higher intensity threshold. Observing the dissociative aspects, the relative positions of the  $1\omega$  and  $2\omega$  peaks are consistent with what we would expect. The  $2\omega$  process is slightly skewed more towards higher intensity than the  $1\omega$  consistent with the need to absorb an extra photon of light (higher photon flux required).

## III. Variation of laser polarization angle

The final observation we report on is that which involves rotation of the linear polarization direction of the laser field. This is done with respect to the detector axis of the spectrometer hence  $0^\circ$  corresponds to parallel to this axis while  $90^\circ$  is orthogonal. Displayed in Figure 3(a) is the forward peaks (centre indicated by black dashed line) of the TOF spectra at the

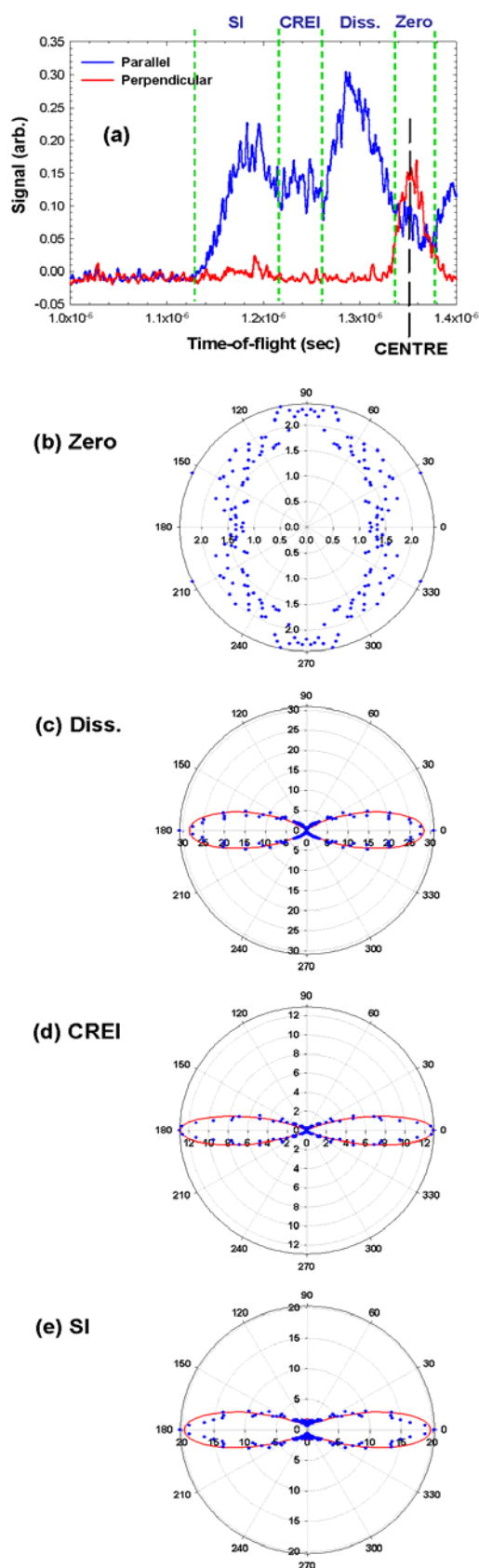


**Figure 3.** Results from rotation of the polarization angle of the laser with respect to the spectrometer detector axis.  $0^\circ$  is parallel to this axis,  $90^\circ$  orthogonal. (a) Forwards peaks from the time-of-flight spectra for both parallel and perpendicular orientation. The labeled peaks correspond to that described in the text. (b)-(e) show polar plots of the integrated signal between the limits identified in (a) for each of the processes Zero, Diss., CREI and SI (blue circles). Fitted to the data in (c)-(e) are  $\cos^n\theta$  distributions (red curves) with  $n=14, 26$  and  $18$  respectively.



two extremes (parallel and perpendicular). The main elements described thus far are again present in the parallel spectrum. To analyze the results we divide the spectrum into four parts, the zero energy peak (Zero), BS dissociation, CREI and SI. The total signal within these boundaries is integrated as a function of the polarization angle and plotted on the polar plots shown in Figures 3(b)-3(e). Fitted to the distributions in 3(c)-3(e) are  $\cos^n\theta$  curves where  $\theta$  is the polarization angle. Due to the small extraction aperture (0.25mm) used for high resolution in the ISS method, the angular acceptance of the spectrometer is small even for low energy fragments. Thus we may not say anything quantitative about the results without correction for this geometrical effect. However even observing the data, a couple of interesting features are apparent. The best  $\cos^n\theta$  fits to the BS, CREI and SI distributions are for  $n = 14, 26$  and  $18$  respectively.

Before making comment on the relative shapes of the distributions, it should be noted that the distributions are clearly much sharper than a  $\cos^2\theta$  distribution i.e. the expected distribution from simply resolving the field component along the linear bond axis. This in itself is strong evidence for field-induced reorientation of either the  $H_2$  neutral molecule or indeed the  $H_2^+$  ion as it dissociates even on an ultrafast timescale. It plays a particularly important role for the BS dissociation and CREI mechanisms as both these processes arise through a multiphoton coupling of  $H_2^+ \Sigma_g$  and  $\Sigma_u$  states, efficient only for molecules aligned parallel to the field<sup>10,11</sup>.

Now as SI is a higher kinetic energy release peak than CREI, the fact that it has a lower  $n$  fit is somewhat surprising. Should the fall off in signal purely be an angular acceptance effect the higher energy process should decline more rapidly with angle increase than CREI. Even more surprising perhaps is observation of the zero energy process. Whilst it is zero energy, rotation of the polarization angle should play no part if we are simply observing geometrical effects. The angular acceptance collects all products as it is only a case of extracting the stationary ions i.e. no off-axis momentum component. In Figure 3(b) there is a clear enhancement in the zero energy peak as the polarization angle rotates towards perpendicular orientation (~80% increase in signal). No previous predictions or experiments showing such an effect have been reported.

### Conclusions and outlook

In summary, we have presented here the first results from the newly installed hollow-fibre compression system producing stabilized 10fs pulses in Astra TA1. Interacting with  $H_2$  and  $D_2$  targets, we observed time-of-flight spectra displaying features similar to those observed in recent ultrashort pulse experiments<sup>15,25</sup> with an additional peak arising at zero energy release. A systematic variation of pulse length through spectral broadening resulted in distinctive changes in both the coulomb explosion and dissociative peaks forming  $H^+/D^+$  ions. However it is somewhat unclear whether the changes in dissociation of  $H_2^+/D_2^+$  are in fact related to the dissociative mechanism itself or simply a product of how the ion is produced. By varying the intensity through an intensity selective scan method the intensity dependence of the major processes is documented. Moreover we show through rotation of the polarization angle an increase in the yield from a zero energy feature as the polarization angle shifts towards perpendicular orientation with respect to the spectrometer axis.

While  $H_2$  and  $D_2$  neutral gas target studies are undoubtedly informative, the most elemental test of  $H_2^+/D_2^+$  dissociative mechanisms is to begin with a prepared target. This defines the initial vibrational state population distribution (Frank-Condon) and using a fast target, collecting the neutral H or D atoms will deconvolute the dissociative processes from any coulomb explosion features simplifying the interpretation. It is such a study that we plan to perform with our ionic beam apparatus<sup>3,4</sup>.

The main difficulty is the low number density of ion beams, typically of the order of  $10^3$  down on a gas target. The restricted volume of interaction further impedes the measurement particularly with the current 10Hz repetition rate of the laser. However with the new planned upgrade of the Astra laser system to a kHz oscillator we shall be in a strong position to carry out the first studies on a  $H_2^+$  target using few-cycle (10fs) pulses.

### References

1. See for example the recent review, J H Posthumus, Rep. Prog. Phys. **67** 623 (2004)
2. X Urbain *et al.*, Phys. Rev. Lett. **92** 163004 (2004)
3. T K Kjeldsen and L B Madson, <http://arxiv.org/>, e-print physics 0501157 (2005)
4. I D Williams *et al.*, J. Phys. B **33** 2743 (2000)
5. W A Bryan *et al.*, CLF Annual Report (2003-04) p58
6. K Sandig *et al.*, Phys. Rev. Lett. **85** 4876 (2000)
7. P H Bucksbaum *et al.*, Phys. Rev. Lett. **64** 1883 (1990)
8. L J Frasinski *et al.*, Phys. Rev. Lett. **83** 3625 (1999)
9. J H Posthumus *et al.*, J. Phys. B **31** L553 (1998)
10. T Zuo and A Bandrauk, Phys. Rev. A **52** R2511 (1995)
11. T Seideman *et al.*, Phys. Rev. Lett. **75** 2819 (1995)
12. Posthumus *et al.*, J. Phys. B **28** L349 (1995)
13. H. Niikura *et al.*, Nature (London) **417**, 917 (2002)
14. H. Sakai *et al.*, Phys. Rev. A **67**, 063404 (2003)
15. F Legare *et al.*, Phys. Rev. Lett. **91** 093002 (2003)
16. A A A El-Zein *et al.*, Phys. Scripta **T92**, 119 (2001)
17. P Hansch and L D V Woerkom, Opt. Lett. **21**, 1286 (1996)
18. W A Bryan *et al.*, CLF Annual Report (2002-03) p67
19. J McKenna *et al.*, CLF Annual Report (2003-04) p64
20. C Cornnaggia *et al.*, Phys. Rev. A **42**, 5464 (1990)
21. W C Wiley and I H McLaren, Rev. Sci. Instrum. **26**, 1150 (1955)
22. M. Nisoli *et al.*, Opt. Lett. **22**, 522 (1997)
23. I C E Turcu *et al.*, CLF Annual Report (2004-05) p223
24. See for example, M R Thompson *et al.*, J. Phys. B **30** 5755 (1997)
25. Rudenko *et al.*, J. Phys. B **38** 487 (2005)